Electronic Structure of Methoxy-, Bromo-, and Nitrobenzene Grafted onto Si(111)

Ralf Hunger,*,† Wolfram Jaegermann,† Alexandra Merson,‡ Yoram Shapira,‡ Christian Pettenkofer,§ and Jörg Rappich||

Institute of Materials Science, Technische Universität Darmstadt, Petersenstr. 23, 64287 Darmstadt, Germany, Department of Physical Electronics, Tel-Aviv University, Ramat-Aviv 69978, Israel, and Abteilung Halbleiterheterogrenzflächen and Abteilung Silizium-Photovoltaik, Hahn-Meitner-Institut Berlin GmbH, Bereich Solarenergieforschung, Glienicker Str. 100, 14109 Berlin, Germany

Received: October 6, 2005; In Final Form: May 15, 2006

The properties of Si(111) surfaces grafted with benzene derivatives were investigated using ultraviolet photoemission spectroscopy (UPS) and X-ray photoelectron spectroscopy (XPS). The investigated materials were nitro-, bromo-, and methoxybenzene layers ($-C_6H_4-X$, with $X = NO_2$, Br, $O-CH_3$) deposited from diazonium salt solutions in a potentiostatic electrochemical process. The UPS spectra of the valence band region are governed by the molecular orbital density of states of the adsorbates, which is modified from the isolated state in the gas phase due to molecule−molecule and molecule−substrate interaction. Depending on the adsorbate, clearly different emission features are observed. The analysis of XPS intensities clearly proves multilayer formation for bromo- and nitrobenzene in agreement with the amount of charge transferred during the grafting process. Methoxybenzene forms only a sub-monolayer coverage. The detailed analysis of binding energy shifts of the XPS emissions for determining the band bending and the secondary electron onset in UPS spectra for determining the work function allow one to discriminate between surface dipole layers—changing the electron affinity—and band bending, affecting only the work function. Thus, complete energy band diagrams of the grafted Si(111) surfaces can be constructed. It was found that silicon surface engineering can be accomplished by the electrochemical grafting process using nitrobenzene and bromobenzene: silicon-derived interface gap states are chemically passivated, and the adsorbate-related surface dipole effects an increase of the electron affinity.

1. Introduction

In the past years, semiconductor surfaces terminated with organic compounds have attracted considerable interest due to the scientific importance of this heterointerface. The application perspectives lie in the engineering possibilities of inorganic semiconductor surfaces[1] and the development of novel hybrid inorganic/organic semiconductor devices.[2] In terms of semiconductor surface engineering, control of the surface state density, tailoring of the electron affinity, and chemical inertness are desirable. An overview of the modification of the surface properties of primarily binary semiconductors by organic surface treatments is given in ref 1. An impressive example for this approach is the tuning of the electron affinity of GaAs by about 1 eV through the adsorption of tartaric acid derivatives where the substituent X on the benzene group allows for a systematic modification of the molecular dipole.[3] For the elemental semiconductor silicon, organic surface functionalization by wet processes was demonstrated by alkylation[4,5] and by electrochemical grafting of aryl groups.[6,7,8] The latter process as developed in refs 6 and 7 is illustrated in Figure 1. By electron injection into a solution of diazonium salt $BF_4N_2-C_6H_4-X$, intermediate aryl radicals $\bullet C_6H_4-X$ are formed (Figure 1a). In a two-step process, one aryl radical abstracts hydrogen from the hydrogen-terminated Si(111) surface and creates a dangling bond (Figure 1b), which reacts with another aryl radical to form a covalently bonded $[Si_3]\equiv Si-C_6H_4-X$ ($X = NO_2$, Br) surface species (Figure 1c and d). Again, by variation of the functional group X, the dipole of the adsorbed molecule can in principle be modified. This was studied by Rappich and co-workers,[8,9] who, in addition to nitro- and bromobenzene, investigated diethylaniline and chloro-, dichloro-, and methoxybenzene for the modification of Si(111) surfaces in an electrochemical grafting process. The dipole moments of aryl radicals were calculated, and their influence on the interface formation process and the electronic properties of the functionalized Si surfaces was discussed.[9] By in situ measurements of the photoluminescence and surface photovoltage, electronic passivation and a change in band bending induced by the aryl termination of the Si surface were demonstrated.[8,9]

In this paper, we investigate the properties of Si(111) surfaces terminated with benzene derivatives by ultraviolet photoelectron spectroscopy (UPS). UPS allows not only for direct and absolute measurements of the work function, but it was found that the molecular electronic structure of the adsorbate could be imaged by UPS and can be employed for a unique identification of the adsorbate. The vacuum adsorption of pure benzene on Si(001)−(2×1) surfaces has been the subject of a number of publications in the past years, including soft-X-ray and ultraviolet photoelectron spectroscopic studies.[10,11] Our data demonstrate that the measurement of the valence electronic structure of organic adsorbates is not limited to vacuum processes but can be applied to the analysis of wet, electrochemical deposition processes performed at atmospheric pressure. The UPS study was combined with X-ray photoelectron spectroscopy (XPS), which

* Corresponding author. E-mail: hunger@surface.tu-darmstadt.de. Mail address: c/o BESSY, Albert-Einstein-Str. 15, 12489 Berlin, Germany.
† Technische Universität Darmstadt.
‡ Tel-Aviv University.
§ Abteilung Halbleiterheterogrenzflächen, Hahn-Meitner-Institut.
|| Abteilung Silizium-Photovoltaik, Hahn-Meitner-Institut.

10.1021/jp055702v CCC: $33.50
Published on Web 07/14/2006

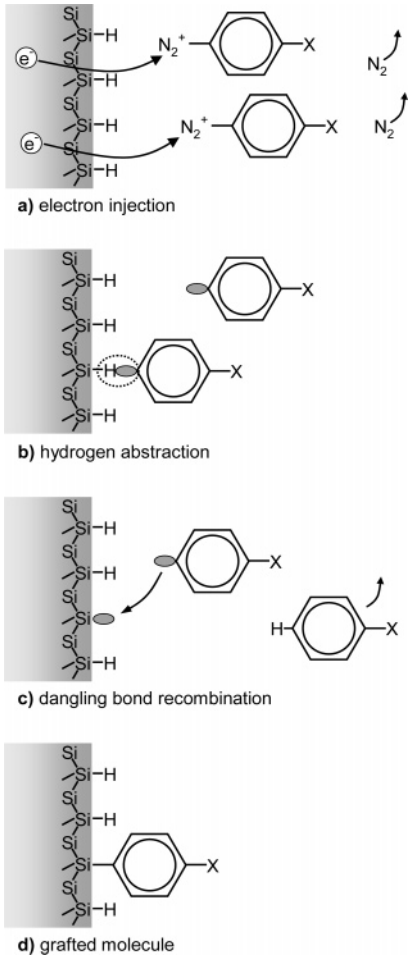

Figure 1. Schematics of the electrochemical grafting process. (a) By electron injection from the working electrode, the bond between the diazo group and the phenyl ring is broken, N_2 is split off, and phenyl radicals are generated. (b) A phenyl radical abstracts hydrogen from the silicon surface and generates a silicon dangling bond. (c) A second phenyl radical recombines with the dangling bond, and (d) a covalent Si−C bond is established between a surface silicon atom and the phenyl. At least two electrons are necessary to bind one phenyl group.

simultaneously provided information on the surface composition, adsorbate layer thickness, and surface band bending. The major advantage of the combination of UPS and XPS information is that the contributions of electron affinity changes, that is, surface dipoles, and band bending can be separated, and thus, complete equilibrium band energy diagrams can be constructed.[12] For this study, we chose to investigate nitro-, bromo-, and methoxybenzene layers ($-C_6H_4-X$, with X = NO_2, Br, $O-CH_3$) on Si(111) because the effective dipole moments of these molecules perpendicular to the Si(111) surface span a wide range from 3.9 D (X = NO_2) to −0.5 D (X = OCH_3).[9] Here, the negative sign of −0.5 D implies that the orientation of the adsorbate dipole moment changes by 180°. The derivatized benzene compounds employed in our study are depicted in Figure 2, together with their molecular dipole moment. With these materials, the concept of surface functionalization by attaching benzene derivatives and tailoring the electron affinity by grafting different functional groups carrying different dipole moments can be favorably tested.

2. Experimental Section

Wafers of p-Si(111) (2.5−5 Ωcm) were cleaned using a standard procedure and thermally oxidized (the thermal oxide

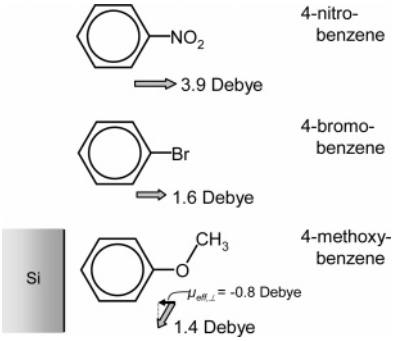

Figure 2. Overview of the benzene derivatives employed for the surface functionalization by electrochemical grafting. The direction and magnitude of the molecular dipole arising from the charge distribution within the derivatized phenyl molecule C_6H_5-X (X = NO_2, Br, OCH_3) is indicated by a gray arrow. For methoxybenzene, the effective dipole moment along the molecule axis which after grafting is perpendicular to the Si surface, $\mu_{eff,\perp}$, has the opposite direction compared to those of nitro- and bromobenzene.

thickness was about 100 nm). The wafers were cut into 20 × 20 mm^2 samples. The samples were ultrasonically cleaned in acetone and water, and the thermal oxide was etched back in 2% HF. Then, a chemical oxide was formed in H_2SO_4/H_2O_2 = 1:1 solution for 10 min. The back contact was made by InGa eutectic after the chemical oxide had been etched using a droplet of 2% HF. The front surface of the sample was not affected by the preparation of the back contact.

4-Nitro, 4-bromo-, and 4-methoxybenzene diazonium tetrafluoroborate were purchased from Aldrich and used as received, without further purification. The concentration of the diazonium compound solutions was 2.5 mM. The electrochemical preparation of the front surface was performed in a single compartment Teflon cell, using a three-electrode configuration (sample, working electrode; Au ring, counter electrode; Au wire, reference electrode). In reference experiments, the potential of the Au electrode was measured to about +0.54 V versus SCE. The sample was mounted into the cell, and the chemical oxide was etched back in NH_4F (40%), such that flat hydrogenated Si(111) terraces were formed.[13] The NH_4F (40%) was then completely pumped out, and 20 mL of 0.01 M H_2SO_4 was added to the cell. Simultaneously, the potential was switched to −1.2 V to ensure that the H-terminated Si surface was not oxidized. Then, 10 mL of the supporting electrolyte was pumped out and 10 mL of the diazonium salt solution in 0.01 M H_2SO_4 was injected into the cell at constant potential, yielding a diazonium salt solution of 1.25 mM in the reaction vessel. Thus, electrochemical grafting of organic molecules occurred. The current−time transients observed were similar to those described in refs 9 and 14. The electrochemical grafting was terminated by observing zero current that showed that the layer deposition was completed. For the electrochemical grafting processes using the diazonium salts of nitro-, bromo-, and methoxybenzene, we observed net charge flows of −0.47 mC/cm^{-2}, −0.72 mC/cm^{-2}, and −0.12 mC/cm^{-3}. The electrode area was 0.25 cm^{-2}.

After the electrochemical preparation, the samples were rinsed in distilled water, dried, and encapsulated in argon filled compartments. After storage for up to 2 days, the samples were clamped onto stainless steel sample holders and immediately introduced into the vacuum system. The total ambient air exposure between preparation and vacuum insertion was about 30 min. The analysis chamber of the vacuum system is equipped with a Phoibos 150 MCD-9 electron analyzer (SPECS). UPS and XPS data were collected with an entrance slit setting of 6 × 20 mm^2, and the medium area lens mode was employed.

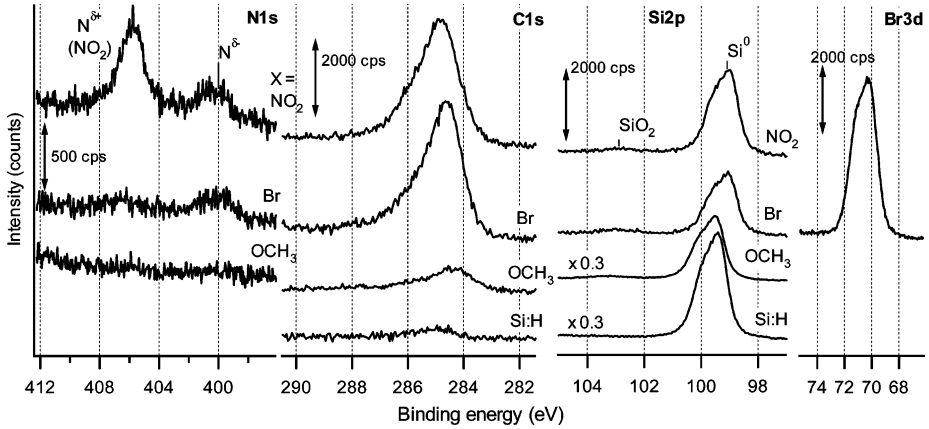

Figure 3. XPS core level spectra of N1s, C1s, Si2p, and Br3d measured on benzene derivative layers C_6H_4-X (X = NO_2, Br, OCH_3) grafted onto Si(111). The XPS spectra of a hydrogen-terminated Si(111) substrate (Si:H) are displayed on the bottom. Note that the Si2p spectra of the methoxy (OCH_3)-benzene deposition and the substrate are scaled down by a factor of 0.3.

The energy scale of the spectrometer was calibrated using the $Au4f_{7/2}$ core level emission at 84.0 eV of a clean, sputtered Au foil. The UPS spectra were excited with a helium UV lamp (Leybold), which produces spectral lines of $h\nu = 21.22$ eV (He I) and 40.82 eV (He II). For the UPS spectra acquisition, a negative bias of -3 eV was applied to the sample to get a clear signal of the secondary electron cutoff. XPS spectra were excited with non-monochromatized Mg Kα radiation ($h\nu = 1253.6$ eV) from an X-ray tube (SPECS). The spectra shown were referenced to the Fermi energy of the samples.

3. Results

(a) XPS Results. After introduction into the vacuum chamber, an XPS survey and detailed spectra were recorded. For reference purposes, in addition to the nitro-, bromo-, and methoxybenzene grafted Si(111) surfaces, a HF(2%)-treated Si(111) substrate was analyzed. The XPS spectra in the core level regions of N1s, C1s, Si2p, and Br3d are displayed in Figure 3. A fluorine F1s emission which would be indicative of BF_4^- remnants was not observed. For the nitro- and bromobenzene processes, the deposition of the organic adsorbate layer is evidenced by the observation of the Br3d core level and the N1s emission at a binding energy, BE, of 406 eV which is characteristic of nitrogen in the environment of a NO_2 group.[15] A substantial increase of the C1s emission was observed compared to the Si(111):H sample, which correlated with a significant attenuation of the substrate Si2p emission. A second N1s component at BE $\sim$ 400 eV was found for the bromo- as well as nitrobenzene process. This signal presumably originated from amino groups (NH_2),[16] which are to be attributed to contaminations of the working solutions. (NH_2 compounds are used as the precursor for the formation of the diazo group and may thus be introduced as contamination of the diazonium salt.) This adventitious nitrogen signal was also observed by other groups.[6,7,17,18] Generally, our findings from XPS are similar to those of refs 6 and 7 where grafting also occurred on Si(111). For the methoxybenzene process, the C1s intensity was much less, indicating a considerably smaller adsorbate layer thickness. A more detailed account of the XPS data will be given in the Discussion section.

(b) UPS Results. Figure 4 shows the He I-excited UPS spectra of Si(111) surfaces grafted with nitrobenzene, bromobenzene, and methoxybenzene. For comparison, the UPS spectrum of the HF-treated Si(111) substrate was included. Depending on the adsorbate, clearly different emission structures are observed. The general structure of He I-excited UPS spectra

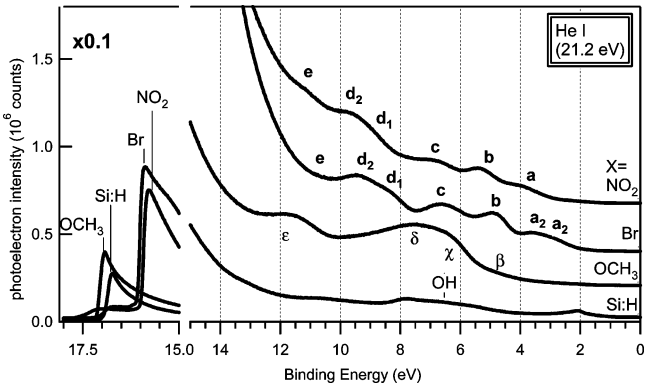

Figure 4. He II-excited UPS spectra of aryl adsorbate layers C_6H_5-X (X = NO_2, Br, OCH_3) grafted onto p-Si(111). The UPS data of a hydrogen-terminated Si(111) substrate are included for comparison ("Si:H"). Characteristic emissions are labeled with roman (a–e) or greek letters ($\beta-\epsilon$). In the region of the secondary electron edge (BE > 15 eV), the spectra are scaled by 0.1. The secondary electron edge marks the work function of the surface. Depending on the adsorbed species, the work function changes by more than 1.0 eV.

is characterized by a strongly increasing background intensity of inelastically scattered photoelectrons (i.e., the so-called secondary electrons). The kinetic energy, KE, of the investigated photoelectrons relates to the binding energy, BE, and the excitation energy, $h\nu$, according to

$$\mathrm{KE} = h\nu - \mathrm{BE} - \mathrm{WF} \qquad (1)$$

with WF being the work function. Hence, for $h\nu - \mathrm{BE} = \mathrm{WF}$, the kinetic energy of the photoelectrons becomes zero and they cannot exit the solid but are reflected at the surface potential barrier of the work function. This produced the sharp intensity drop in the He I spectra for binding energies around 16 eV, which is the so-called secondary electron edge. By its energy position, $\mathrm{BE}(E_{\mathrm{sec}})$, the work function of the investigated surface is determined according to $\mathrm{WF} = h\nu - \mathrm{BE}(E_{\mathrm{sec}})$ as $\mathrm{KE}(E_{\mathrm{sec}}) = 0$. Figure 4 shows that the secondary electron edges of the investigated samples varied from 17.1 to 16.0 eV; hence, the work function, WF, changed from 4.1 to 5.2 eV, that is, by more than 1 eV. The absolute values of the work function are given in Table 1. This change of the work function of Si is supposedly induced by the different functional groups, which carry different molecular dipole moments. The work function of a semiconductor, however, is not solely determined by the electron affinity but also by the position of the Fermi level at the surface, which may be shifted by the occupation of surface

TABLE 1: Surface Electronic Properties of Aryl Adsorbate Layers Grafted onto Si(111)

Si(111)−X adsorbate X =	work function, WF (eV)	binding energy, BE(Si2p$_{3/2}$) (eV)	E_{vbm} (eV)	surface band bending,[c] eV_{bb} (eV)	electron affinity,[d] χ (eV)	surface potential step,[e] δ (eV)
H(/OH)	4.22	99.40	0.68[a]	0.47	3.78	−0.27
Ph-NO_2	5.23	99.01	0.30[b]	0.09	4.41	0.36
Ph-Br	5.13	99.06	0.34[b]	0.13	4.35	0.30
Ph-OCH_3	4.06	99.49	0.78[b]	0.57	3.72	−0.33
uncertainty	±0.10	±0.05	±0.05	±0.05	±0.15	±0.15

[a] Determined from the defined emission onset in HeII-excited UPS spectra. Therefrom, the binding energy with respect to the valence band maximum energy, BE^v(Si2p), was determined according to BE^v(Si2p) = BE(Si2p) − E_{vbm} = 98.71(10) eV in good agreement with ref 37. [b] Calculated according to E_{vbm} = BE(Si2p) − BE^v(Si2p). [c] Calculated according to $eV_{bb} = E_{vbm} - |E_{vb} - E_F|_{vol}$. The bulk doping of the Si substrate yields $|E_{vb} - E_F|_{vol}$ = 0.21 eV. [d] χ = WF + E_{vbm} − E_g. [e] $\delta = \chi - \chi_{Si}$. As the bulk electron affinity of silicon, χ_{Si} = 4.05 eV was used.[36]

TABLE 2: Emission Features in the UPS Spectra of Aryl Adsorbate Layers C_6H_5

adsorbate	emission label	binding energy, BE,[a] (eV)
X = −NO_2	a	3.90
	b	5.30
	d_1	8.82
	d_2	9.58
	e	10.8
X = −Br	a_1	2.85
	a_2	3.55
	b	4.85
	d_1	8.29
	d_2	9.39
	e	10.8
X = −OCH_3	β	4.7
	δ	7.5
	ϵ	11.5

[a] Observed binding energy with respect to the Fermi level.

states in the forbidden gap. These two contributions can be separated by combining information derived from UPS and XPS. This will be undertaken below in part c of the Discussion section.

In the valence band region, that is, for binding energies up to 14 eV, the UPS spectra exhibit characteristic emission features that differ for the various adsorbates. The UPS spectrum of the Si(111)−C_6H_4−NO_2 surface exhibits emission features at 3.9, 5.3, 6.8, 9.6, and 11.2 eV, respectively, labeled a−e in Figure 2. The valence band of Si(111)−C_6H_4−Br is characterized by emissions at 2.9/3.5 eV, 4.9 eV, 6.7 eV, 8.3/9.4 eV, and 10.8 eV. The Si(111)−C_6H_4−OCH_3 surface exhibits emission features at 4.7, 6.3, 7.5, and 11.5 eV. Apparently, the different molecular adsorbates give rise to specific photoemission features in the valence band region. The binding energies of the observed emission features were evaluated by the second derivative of the spectra and were listed in Table 2.

(c) Comparison of Adsorbed State and Gas Phase. To a first approximation, the angle-integrated UPS spectra reflect the density of states (DOS) in the valence band region.[19] In the case of molecular adsorbates, the DOS is governed by the molecular orbitals, which can—depending on the interaction of the adsorbate with its environment—be modified from the isolated state in the gas phase. Literature data of the benzene derivatives in the gas phase investigated by UPS are available for bromobenzene[20] and nitrobenzene.[21] In Figure 5, these gas phase He I spectra are compared to UPS spectra of the solid adsorbate layers of nitro- and bromobenzene, excited with He I and He II radiation, respectively. In Figure 5a and c, the gas phase spectra of nitro- and bromobenzene, which were taken from refs 20 and 21, were plotted. Below the spectra of the adsorbate layers in Figure 5b and d, the measured binding energies of the emission features a/a_1,a_2 to e are indicated by vertical bars. In the gas phase data, 11 respectively 12 different molecular orbitals were identified and assigned by a comparison

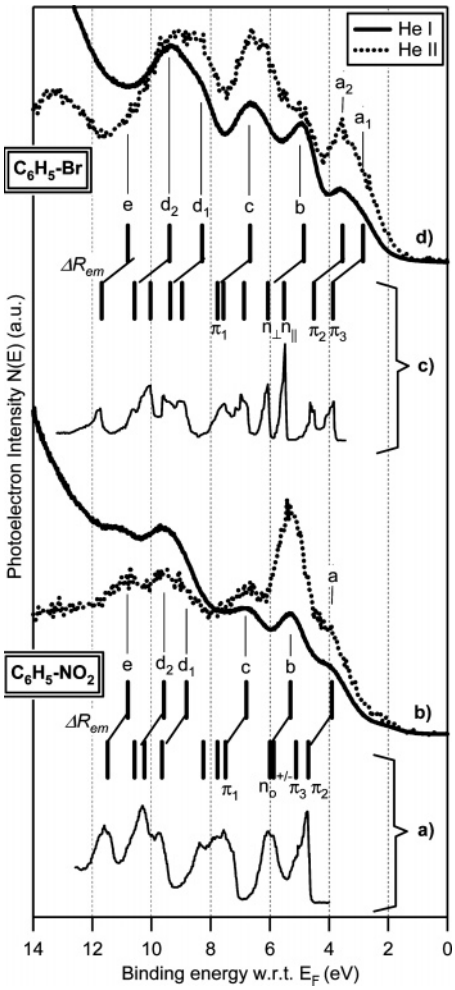

Figure 5. Comparison of the He I- and He II-excited UPS spectra of (b) nitrobenzene (C_6H_5−NO_2) and (d) bromobenzene (C_6H_5−Br) layers grafted onto Si(111) with the respective gas phase data (a, c). The gas phase spectra are reproduced from refs 20 and 21, and the ionization potentials of assigned molecular orbitals are indicated by vertical bars. The gas phase data are referenced to the Fermi level of the respective adsorbate layer using the measured work function, WF. The molecular IPs are shifted by additional extramolecular screening, ΔR_{em}, to lower the binding energy.

to molecular orbital calculations. The ionization potentials, IPs, of these molecular orbitals are indicated as vertical bars in Figure 5a and c. The molecular orbitals can be grouped into π-bonding-related orbitals of the benzene ring (π_i), filled, lone-pair-like orbitals of the functional groups NO_2 or Br (denoted as n), and σ-bond-derived orbitals (nonlabeled). Gas phase spectra are commonly referenced to the vacuum level, and binding energies are denoted as ionization potentials, IPs, of the respective molecular orbital, which is the binding energy with respect to

the vacuum level. Solid state valence band spectra, however, are commonly referenced to the Fermi level. These energy scales are related by

$$\mathrm{BE} = \mathrm{IP} - \mathrm{WF} \tag{2}$$

and the measured work functions of the grafted nitro- and bromobenzene layers have been used. The similarity of the emission features in the adsorbed solid state or the gas phase is obvious. Due to additional phonon broadening in the solid state, the individual orbital contributions are broadened; hence, not all emission features of the gas phase are resolved.

The molecular orbital binding energies of the adsorbed state are shifted to smaller binding energies than in the gas phase. This shift, ΔR_{em}, amounts to 0.69(5) and 1.01(5) eV for nitro- and bromobenzene layers grafted onto Si(111), respectively. This apparent shift of binding energies between the gas phase and adsorbed solid state results from the differing screening environments of the two states. In the photoemission process, a positively charged photohole is created. In the adsorbed solid state, the neighboring molecules contribute to the screening of this positive charge by rearrangement of the valence electrons. There is an additional extramolecular screening of the photohole, which reduces the Coulomb attraction between photoelectron and photohole and gives rise to an apparent lower binding energy. The latter is lowered by the extramolecular relaxation energy, ΔR_{em}, compared to the isolated gas phase photoemission process.[19]

4. Discussion

(a) Electronic Structure of the Adsorbate Layers. The good correspondence between the emission features of the gas phase and the adsorbed, electrochemically grafted, solid surface layer reflects the success of the electrochemical grafting procedure for nitro- and bromobenzene. On the basis of the good agreement between the adsorbed state and gas phase data, it is reasonable to assume that the emission structures originate from the same molecular orbitals. Hence, the assignment derived from the gas phase data can be transferred to the adsorbed phase: The delocalized π states of the benzene rings having smaller binding energies than the σ-derived bands are common to both adsorbate systems, nitro- and bromobenzene. The emission feature a or a_1 is the highest occupied molecular orbital (HOMO) and consists of a π_2 or π_3 state (a_1 or b_2 symmetry) for nitro- and bromobenzene, respectively.[20,21] The emission structure c corresponds to the π_1 orbital. The emission features d_1/d_2 and e involve σ-bond-derived molecular orbitals predominantly on the benzene rings. The prominent emission b of the adsorbate layers corresponds to molecular orbitals on the functional group NO_2 or Br, respectively. In analogy to refs 20 and 21, they are labeled $n_\perp$, $n_\parallel$ and n_0^+, n_0^-.

The assignment of the structures b as being due to the functional groups NO_2 and Br is further supported by the energy-dependent photoionization cross sections. Comparing the He I- and He II-excited spectra, the relative intensity of b is significantly increased for He II excitation in the case of nitrobenzene. For bromobenzene, however, structure b is significantly less pronounced for He II excitation. This is a result of the energy dependence of the atomic photoionization cross section, σ, of the respective orbitals: Whereas the relative cross section of the N2p orbitals increases from $\sigma(\mathrm{N2p})/\sigma(\mathrm{C2p}) = 1.6$ to 2.3 when going from He I ($h\nu = 21.2$ eV) to He II excitation ($h\nu = 40.8$ eV), the relative cross section of Br2p, $\sigma(\mathrm{Br2p})/\sigma(\mathrm{C2p})$ decreases from 2.5 to 0.5.[22] The $n_\parallel/n_\perp$ orbitals (lone pairs) of the Br ligand exhibit a clear energy splitting in the gas phase; however, in the adsorbed layer, only a single emission line is observed. A preferential orientation of the adsorbed molecules in conjunction with dipole selection rules might explain the absence of the $n_\parallel$ emission; however, more detailed angle-dependent measurements would be necessary to corroborate this explanation.

The UPS spectrum of the sample that was subjected to the grafting process using a methoxybenzene diazonium salt closely resembles that of thin electrochemical oxides formed on Si(111).[23] The emissions χ, δ, and ϵ are attributed to the O2p orbitals in OH (χ) and SiO_{2-x} (δ, ϵ), respectively. The O2p emissions from methoxybenzene, $C_6H_5-OCH_3$, however, are expected in the same energy range. The weak emission, β, can be related to the π_2/π_3 emission bands (C2p derived) of methoxybenzene according to the comparison to the UPS data of solid multilayers of $C_6H_5-OCH_3$ on TiO_2.[24] In consequence, the valence band features of the methoxybenzene grafted sample are dominated by silicon oxide/hydroxide-like emissions; however, they are consistent with a sub-monolayer coverage of methoxybenzene which would contribute with only minor intensity to the total spectrum. This conclusion is supported by an analysis of the intensities of the XPS core levels.

(b) Thickness Estimation from XPS. To estimate the thickness of the deposited aryl layers, the intensity of the C1s and bulk $Si2p^0$ core level emissions in XPS was evaluated. For the nitro- and bromobenzene grafted surfaces, $C1s/Si2p^0$ intensity ratios of 2.5 and 3.4 were found, respectively. The same intensity ratio of the sample subjected to the methoxybenzene grafting process was only 0.2 (cf. Figure 3). Qualitatively, this means that the deposited bromo- and nitrobenzene layers were considerably thicker than that of the methoxybenzene process.

For a quantitative estimate, the closed overlayer model was applied.[25] The thickness of the adsorbed overlayers was estimated from the relative intensities of the aryl C1s and substrate Si2p emissions, $I_{\mathrm{C1s}}/I_{\mathrm{Si2p}}$. The substrate and overlayer photoelectron intensities depend on the overlayer thickness, d, according to

$$\frac{I_{\mathrm{C1s}}}{I_{\mathrm{Si2p}}}(d) = \frac{I^{\infty}_{\mathrm{C1s}}[1 - \exp(-d/\lambda^{\mathrm{o}}_{\mathrm{C1s}})]}{I^{\infty}_{\mathrm{Si2p}} \quad \exp(-d/\lambda^{\mathrm{o}}_{\mathrm{Si2p}})} \tag{3}$$

where $I^{\infty}_{\mathrm{Si2p}}$ is the photoelectron intensity of a clean, semi-infinite silicon crystal, $I^{\infty}_{\mathrm{C1s}}$ would be the C1s photoelectron intensity of a semi-infinite, solid layer of the respective benzene derivative, $\lambda^{\mathrm{o}}_{\mathrm{C1s(Si2p)}}$ is the electron mean free path, λ, of C1s(Si2p) photoelectrons *in* the overlayer (o). $\lambda^{\mathrm{o}}_{\mathrm{C1s}}$ and $\lambda^{\mathrm{o}}_{\mathrm{Si2p}}$ were approximated by calculated data of the structurally related solid polystyrene[26] with $\lambda^{\mathrm{o}}_{\mathrm{C1s}} = 3.2$ nm and $\lambda^{\mathrm{o}}_{\mathrm{Si2p}} = 3.6$ nm. Following ref 27, the intensities $I^{\mathrm{inf}}_{\mathrm{C1s}}$ and $I^{\mathrm{inf}}_{\mathrm{Si2p}}$ were estimated according to

$$I^{\infty}_{\mathrm{X}} = \mathrm{const}\cdot n_{\mathrm{X}}\cdot\sigma_{\mathrm{X}}\cdot\lambda_{\mathrm{X}}\cdot T(\mathrm{KE_X}) \tag{4}$$

with X = C1s and Si2p and where n_{X} denotes the elemental density, T(KE) is the transmission function of the analyzer, and σ is the photoionization cross section. The elemental density, n_{C}, of carbon in the adsorbed aryl layer was approximated by that of the pure liquid compound. Due to the discrepancies in the values for σ in the literature,[22,28] a considerable uncertainty was introduced into the estimation. Depending on the photoionization cross sections assumed, the ratio $I^{\infty}_{\mathrm{C1s}}/I^{\infty}_{\mathrm{Si2p}}$ varied from 2.2 to ~1.0. Finally, the overlayer thickness, d, was derived from the experimental $I_{\mathrm{C1s}}/I_{\mathrm{Si2p}}$ ratio by applying the described

TABLE 3: Comparison of Aryl Radical Generation and Layer Thickness for Grafting Processes with $N_2C_6H_4-X$ ($X = NO_2$, Br, OCH_3)

	X =		
	NO_2	Br	$O-CH_3$
charge, q, per unit area (mC/cm^2)	−0.47	−0.72	−0.12
radicals per unit area ($10^{15}/cm^2$)	2.9	4.5	0.7
radicals per adsorbate site,[a] n_X	8	12	2
XPS intensity ratio C1s/Si2p	2.5	3.4	0.2
film thickness (low−high)[b] (nm)	2.7−4.5	3.4−5.3	0.25−0.5
film thickness (low−high)[c] (ML)	4−7	5−8	0.4−0.7
grafting yield[d]	0.5−0.9	0.4−0.7	0.2−0.4

[a] One adsorption site is defined as the surface unit mesh of a $(1\times\sqrt{3})$R30° superstructure comprising two silicon surface atoms. The adsorption site density on Si(111) is 3.9×10^{14} cm^{-2}. [b] The low−high range is given by the application of $I^{\infty}_{C1s}/I^{\infty}_{Si2p} = 2.2$ and 1.0, respectively, in eq 3, which result from diverging calculated photoionization cross sections. [c] One monolayer (ML) is defined as one adsorbed molecule per adsorption site. Its thickness was assumed as 0.67 nm. [d] Average number of surface attached phenyls per injected electron.

figures to eq 3. Eventually, for the nitro- and bromobenzene layers, an adsorbate thickness of 3−5 nm is estimated. Assuming the thickness of one monolayer (ML) of an aryl adsorbate is about 0.7 nm[6] the calculated thickness translates into 4−8 monolayers for nitro- and bromobenzene. For the sample subjected to the grafting process with methoxybenzene, a nominal thickness of only 0.3−0.5 nm is deduced, that is, considerably less than one monolayer. The thickness estimation of the deposited aryl films based on the XPS data is given in rows 4−6 of Table 3, where the range of nominal thicknesses is given by the use of 2.2 (low) or 1.0 (high) for $I^{\infty}_{C1s}/I^{\infty}_{Si2p}$. Assuming a monolayer thickness of 0.67 nm[7] for all deposits, the thickness is converted to equivalent monolayers in the fifth row of Table 3.

(c) Multilayer Formation−Surface Polymerization. The thickness of electrografted nitro- or bromobenzene films was evaluated in the literature with different experimental approaches such as an atomic force microscopy (AFM) scratching technique,[29,30] Rutherford backscattering spectroscopy (RBS),[31] and XPS,[18] as in the present study. For nitrobenzene electrografted onto a carbon surface, a layer thickness of 2−4 nm was reported on the basis of AFM.[30,32] Bromobenzene layers grafted onto silicon were found to be up to 2.5 nm thick when deposited under high overpotential, as determined by RBS.[31] The thickness measurement of nitrobenzene layers grafted onto metal surfaces yielded values between 3 and 6 nm.[18] Our observation of multilayer formation with layer thicknesses between ∼3 and ∼5 nm is thus consistent with the literature. Allongue et al. had termed this process, the further attachment of aryls to the surface after the completion of the first monolayer, surface polymerization.[31] In fact, polymeric aryl fragments have been observed in time-of-flight secondary ion mass spectroscopy (ToF-SIMS) experiments from electrografted, multilayered bromo- and nitrobenzene films on carbon.[33] On the basis of these results, the well-known aromatic homolytic substitution (S_H) reaction was proposed as a reaction mechanism leading to multilayer formation.[33,34]

In the following, the phenyl layer thickness determined from XPS is compared to the amount of electrical charge consumed during the potentiostatic grafting process. The first row of Table 3 gives the total cumulative net charge, q, per unit surface area which passed through the working electrode (area 0.25 cm^2). Assuming that every electron transferred into the electrolyte generates one aryl radical, the number of aryl radicals generated per unit area is easily calculated by $q/1.6 \times 10^{-19}$ C in the second row. In the idealized process,[7] the initial grafting process on Si(111) leads to the covalent bonding of one aryl group for every two silicon surface atoms. Due to steric constraints, a higher packing density is unlikely.[31] Thus, we define here one monolayer of aryl adsorbate equivalent to one adsorbed molecule per two silicon surface atoms with a density, $n_{Si(1\times\sqrt{3})R30°}$, of 3.9×10^{14} cm^{-2} (the surface density of Si(111) is 7.8×10^{14} cm^{-2}). This monolayer is standing upright on the Si(111) surface with the aromatic ring plane parallel to {1−10} forming a rectangular $(1\times\sqrt{3})$R30° superstructure on Si(111).[31] The thickness of one monolayer corresponds to 0.67 nm for bromobenzene.[31] Interestingly, the molecular volume of the adsorbed molecule of 0.172 nm^3 is almost identical to the liquid state (0.174 nm^3). Normalization of the number of aryl radicals generated per unit area to the density of molecular adsorption sites, $n_{Si(1\times\sqrt{3})R30°}$, yields the number of aryl radicals per adsorption site, n_X, generated in the whole process. In the initial adsorption process of the first monolayer, n_X should be 2, because two aryl radicals are necessary for the grafting process: The first aryl radical abstracts hydrogen from a silicon surface site, and the second attaches to the generated Si dangling bond. The values of n_X for nitro- and bromobenzene in Table 3 are much higher, approximately 8 or 12, respectively, indicating that in the corresponding processes much more aryl radicals had been generated than necessary for the deposition of single monolayer. This agrees with and corroborates the results of the XPS thickness determination where 4−8 ML thick multilayers instead of single monolayers were deduced.

Eventually, in the last row of Table 3, the number of injected electrons per adsorption site is related to the number of deposited molecules per adsorption site, that is, the number of monolayers, by forming the ratio of these two. This figure is the grafting yield or grafting efficiency. If this number is unity, then for every electron injected into the electrolyte one aryl group is attached to the surface. If electrons or radicals are "lost" in side reactions not leading to aryl attachment, then this number gets smaller than unity. For the monolayer attachment process on Si(111) as depicted in Figure 1, the grafting yield is 0.5, because for the attachment of one phenyl the injection of two electrons (and generation of two radicals) is necessary. Even though there is quite some uncertainty in the data, two points may be noted:

(i) The grafting yields for nitro- and bromobenzene multilayers on Si(111) are rather similar and cluster around ∼0.5. (A similarly prepared Si(111)/$C_6H_4-NO_2$ sample yielded values of 0.4−0.7.) These grafting yields are similar to those of nitrobenzene monolayers grafted onto glassy carbon and highly oriented pyrolytic graphite (HOPG) that had been estimated previously.[35] There, grafting yields of 0.56 (HOPG) and 0.84 (glassy carbon), comparable values to the value 0.5 for multilayers on Si(111) in the present study, had been reported. The uncertainty in the measured grafting yields prevents one from drawing more detailed conclusions on the prevailing reaction mechanisms but appears as an interesting analytical tool for future studies.

(2) The grafting yield for methoxybenzene is about a factor of 2 smaller than that for nitro- or bromobenzene. Even though the aryl generation ratio would be sufficient for the deposition of the first monolayer, the XPS data indicate an organic layer with a thickness of less than 0.5 nm. A fundamental difference between nitro-/bromobenzene on one hand and methoxybenzene on the other hand lies in the orientation of the electrostatic dipole associated with the charge distribution within the aryl radical, as indicated in Figure 6. The situation immediately after electron injection and detachment of the N_2 group is shown. The dipole

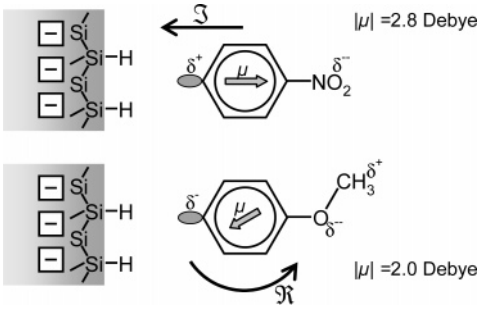

Figure 6. Illustration of the mechanical forces acting on nitrobenzene and methoxybenzene radicals in the electric field of the Helmholtz double layer. The charge distribution within the radicals was computed in ref 9 and is indicated by partial charges, $\delta^{-/+}$, which cause a dipole moment, μ, of the radicals that is indicated by the gray arrow. The electric field in the double layer causes an attractive force, $\mathcal{T}$, on the nitrobenzene radical, whereas a torsional moment, $\mathcal{R}$, is exerted on the methoxybenzene radical, which turns the reactive nonsaturated carbon bond away from the electrode.

moment, μ, generated by the charge distribution within the aryl radical was calculated by Hartig et al.[9] and is indicated by an arrow. For the bromo- and nitrobenzene radicals, the electrostatic charge distribution is such that the end of the nonpaired orbital is further attracted toward the negatively biased electrode (attractive translatory force, $\mathcal{T}$) which is a favorable situation for bonding to the working electrode. On the other hand, the electrostatic charge distribution in the methoxybenzene is such that the radical side becomes negatively charged. This implies that immediately after the release of the N_2 group, a torsional moment, $\mathcal{R}$, acts on the methoxybenzene radical, which turns the CH_3 end group toward the electrode and pushes the reactive, nonpaired orbital away from the electrode. The resulting orientation of the radical prevents the covalent bonding to the working electrode but favors side reactions that lead to an annihilation of the radical. The issue of side reactions during the electrochemical process is discussed in detail in ref 14. This mechanism is the presumable cause for the inefficiency of the grafting process of methoxybenzene.

The proposed reaction mechanism for nitro- and bromobenzene has consequences for the molecular orientation within the adsorbate layer. Whereas the first adsorbed phenyl layer is believed to be standing upright with respect to the Si(111) surface, the angle between the ring plane within the second adsorbed phenyl layer is only about 30° and steric problems occur.[31] For even higher film thicknesses, much more molecular orientations become possible, and a continuous loss of molecular orientation can be expected with increasing distance from the interface. As each of the phenyl molecules is associated with an electrostatic dipole, the ordering and disordering of the molecular orientation has consequences for the macroscopic dipole field of the adsorbate layer. The electronic surface potentials are discussed in detail in the following section.

(d) Surface Potentials—Band Bending. The work function of the investigated samples, measured by the position of the secondary electron edge in Figure 4, varied by more than 1 eV depending on the diazonium salt used. Generally, this shift is attributed to the potential step, δ, associated with the dipole moment of the deposited organic molecule. This desired property allows for the tailoring of the electron affinity. A change in the electron affinity, χ, however, is not the only possible cause for a shift of the work function, WF. This is illustrated in the surface energy band diagram of Figure 7, where the relevant surface potentials are indicated. In the case of a semiconductor, surface band bending, eV_{bb}, can occur, which shifts the Fermi level at

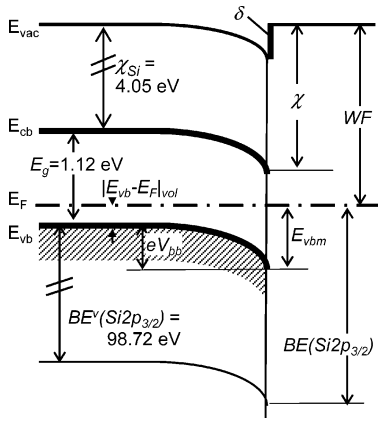

Figure 7. Energy band diagram of a functionalized silicon surface with band bending, eV_{bb}, and a surface dipole, δ, modifying the intrinsic electron affinity of silicon, χ_{Si}. eV_{bb} is derived from the measurement of the $Si2p_{3/2}$ core level binding energy, BE, and then, δ is determined from eV_{bb} and the work function, WF.

the semiconductor surface. This causes a change in the work function even without any change of the electron affinity, χ, which implies that, in order to investigate the potential step induced by the adsorbed layer, the band bending of the semiconductor must be known. Band bending does indeed play a role in the investigated layers, as is apparent from Figure 3, where—depending on the phenyl adsorbate—clearly different BEs of the substrate Si2p emission are observed.

The work function, WF, is defined as the energy difference between the vacuum level, E_{vac}, and the Fermi level, E_F. The position of the Fermi level above the valence band maximum, E_{vb}, at the surface is denoted as E_{vbm}. Then,

$$\mathrm{WF} = E_g - E_{vbm} + \chi \tag{5}$$

where χ is the measured electron affinity of the surface. The effect of an adsorbate or surface termination layer can be viewed such that the "intrinsic electron affinity" of Si, χ_{Si}, which is a constant, is modified by a dipole contribution, δ, which depends on the charge distribution at the interface and within the adsorbate layer:[3]

$$\chi = \chi_{Si} + \delta \tag{6}$$

With the potential step, δ, defined such that an increase of the electron affinity corresponds to $\delta > 0$, WF can be written as

$$\mathrm{WF} = (E_g - E_{vbm}) + (\chi_{Si} + \delta) \tag{7}$$

where E_g is the band gap of silicon, 1.12 eV.[36] On the other hand, E_{vbm} can be expressed by the Fermi level position in the bulk, $|E_{vb} - E_F|_{vol}$, and the surface band bending, eV_{bb}:

$$E_{vbm} = |E_{vb} - E_F|_{vol} + eV_{bb} \tag{8}$$

Finally, eq 7 can be rearranged to give an equation for the surface potential step, δ, which contains only known constants or measured quantities:

$$\delta = \mathrm{WF} - E_g - \chi_{Si} + E_{vbm} \tag{9}$$

The position of the Fermi level at the silicon surface can be derived from the observed binding energy, BE(Si2p), of the $Si2p_{3/2}$ emission, which is determined by curve fitting of a single component Voigt profile doublet to the measured spectra. The

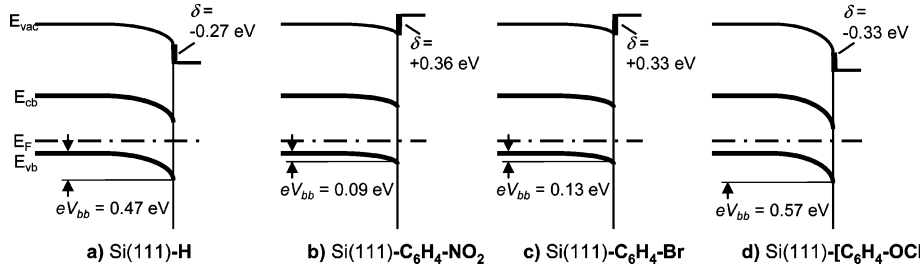

Figure 8. Energy band diagrams of the investigated surfaces: (a) HF-treated, hydrogen-terminated p-Si(111)−H with traces of OH; (b) nitrobenzene grafted onto p-Si(111); (c) bromobenzene/p-Si(111); (d) methoxybenzene/p-Si(111). The biggest surface dipole and simultaneously lowest surface band bending are obtained for part b, while part d yields a surface dipole of opposite sign and a considerable surface band bending of approximately 0.6 eV.

binding energy of Si2p with respect to the valence band maximum

$$\mathrm{BE^v(Si2p)} = \mathrm{BE(Si2p)} - E_{\mathrm{vbm}} \qquad (10)$$

is a constant and independent from the surface band bending (cf. Figure 7). $\mathrm{BE^v(Si2p)}$ was determined for the hydrogen-terminated reference sample as the energy difference between the measured core level BE and the steep emission onset at the valence band edge in He II-excited spectra (not shown), which yielded $E_{\mathrm{vbm}} = 0.68(5)$ eV. A value of $\mathrm{BE^v(Si2p)} = 98.71(10)$ eV was determined which agrees well with literature values (98.74(4) eV[37]). For the phenyl adsorbate layers, E_{vbm} was then calculated according to eq 10.

The surface electronic properties were calculated for the hydrogen-terminated reference substrate and the phenyl adsorbate layers from the experimental data of the work function, WF, and BE(Si2p) as described above. The results are listed in Table 1. Using the derived numerical values, the corresponding surface energy band diagrams were constructed in Figure 8. For the adsorbate multilayers of nitro- and bromobenzene, the observed band bending, eV_{bb}, is small with only ∼0.1 eV; hence, these surfaces are close to the flat-band condition. For both surfaces, the electron affinity, χ, is increased. This increase is attributed to the dipole contribution of the adsorbate layer. The potential step, δ, associated with the adsorbate layers is +0.36(15) and +0.33(15) eV for Ph−NO_2 and Ph−Br multilayers, respectively. For the HF-treated Si(111) surface, a comparatively high band bending of about 0.5 eV was observed which indicates that the hydrogen termination was not perfect, because in this case flat-band conditions would have been observed. [In our experience, $E_{\mathrm{vbm}} \sim 0.7$ eV is the usual pinning position for partially oxidized Si(111):H surfaces. The surface states responsible for this Fermi level pinning can be attributed to oxygen in the back-bonds of the outermost Si surface atoms.[38] For the substrates employed with a bulk dopant density of about 4×10^{15} $\mathrm{cm^3}$, a surface state density of 10^{-4} ML is sufficient to effect the observed band bending of 0.5 eV which explains why a corresponding SiO_2 emission is not observed in the Si2p XPS signal (Figure 3).] The emission at about BE = 6.8 eV in the HeI UPS spectrum is typical for O2p in OH groups, indicating as well a partial OH termination of the HF-treated sample.[39] The surface potential step, δ, of this surface is −0.27(10) eV, implying that the electron affinity is lowered by the imperfect hydrogen termination.

The surface potentials of the silicon surface subjected to the grafting process with methoxybenzene were similar to that of the imperfect hydrogen termination. In particular, a rather high band bending, eV_{bb}, of ∼0.6 eV was found, as well as a lowering of the surface electron affinity by $\delta = -0.32(15)$ eV.

(e) Tailoring of the Electron Affinity. The desired functions of the organic adsorbate layer in terms of functionalization of silicon surfaces are twofold:[1] (i) chemical and electronic passivation of surface gap states by covalent bonding to the silicon surface and (ii) tuning of the electron affinity by the dipole contribution of the adsorbate. Both functions are fulfilled by the nitro- and bromobenzene multilayers deposited in the electrochemical grafting process. The resulting surfaces are close to flat-band conditions with a remaining surface band bending of only ∼0.1 eV. This is in agreement with in situ photovoltage measurements[8,9] where a reduction of band bending was observed. The charge distribution within the interface and the adsorbate layer effects an increase in the electron affinity by an effective potential step of +0.3 to +0.4 eV. Generally, this effective dipole moment is attributed to the dipole contributions of the individual adsorbate molecules which due to their ordering give rise to a macroscopic electrostatic potential step across the adsorbate layer. This is consistent with the dipole moments of covalently bonded nitro- and bromobenzene which were calculated to be 3.9 and 1.6 D, respectively.[9]

In the case of a covalently bonded methoxybenzene molecule with a covalent Si−C bond at the 4-position of the phenyl ring, the projection of the molecular dipole on the surface normal would give an effective dipole moment, $\mu_{\perp,\mathrm{eff}}$, of −0.5 D,[9] where the negative sign indicates the opposite orientation with respect to nitro- and bromobenzene (cf. Figure 2). Hence, a lowering of the surface electron affinity would result. Such an effect was indeed observed for the sample subjected to the electrochemical polarization in methoxybenzene diazonium solution with an effective dipole moment contribution, δ, of about −0.3 eV. The XPS quantification estimated the amount of organic material on the surface to about 0.5 ML equivalents of methoxybenzene. The UPS analysis indicated at the same time a considerable nonintended oxidation and SiO_x formation at the surface during the electrochemical processing. The defects associated with the oxide formation are the presumable reason for the substantial band bending at this surface of ∼0.6 eV. Hence, the desired electronic passivation of the surface was not achieved by the methoxybenzene process. The second function, a reduction of the surface electron affinity, was indeed observed, and the surface dipole was quantified to −0.3 eV. With the present experiments, it cannot be decided, however, to what extent the concurring phenomena of methoxybenzene attachment and surface oxidation contribute to this alteration.

In conclusion, the electrochemical grafting process is effective for nitrobenzene and bromobenzene with the desired surface functionalization and passivation. Further process development should focus on the suppression of multilayer formation, because both functions, modification of the electron affinity and passivation by covalent bonding, are governed by the first monolayer

adsorbate only. The surface functionalization of silicon by the electrochemical grafting of methoxybenzene could not be evidenced as clearly as that for bromo- and nitrobenzene. A much lower grafting yield was observed which was explained by the unfavorable molecular "mechanics" of the grafting process for methoxybenzene radicals. Due to the only partial surface coverage, the distinction between the effects of methoxybenzene-related functionalization and concurring surface oxidation is difficult. In further developments, the process should be refined such that the nonintended, concurring surface oxidation is suppressed and complete monolayers or even multilayers are deposited. In a further step, the effectivity of the electrografted, functionalized phenyl layers for the modification of device characteristics such as Schottky barrier heights should be investigated.

5. Summary

Methoxy-, bromo-, and nitrobenzene layers grafted onto silicon (111) surfaces by cathodic polarization in diazonium salt solutions were investigated in a comprehensive, combined UPS/XPS analysis. The XPS core level signals indicated the deposition of nitro- and bromobenzene multilayers with a thickness between 3 and 5 nm. Balancing the injected charges during electrochemical polarization with the amount of deposited material, a grafting yield of ~0.5 was evaluated for bromo- and nitrobenzene. For methoxybenzene, only a sub-monolayer coverage and a much lower grafting yield was observed. The presumable reason for the difference in grafting efficiency between nitro-/bromo- and methoxybenzene is the different orientations of the dipole moment associated with the intermediate aryl radicals formed. For a more detailed understanding of these steric, orientational effects, further studies by orientation-indicative methods such as IR ellipsometry[40] are necessary. It was demonstrated recently for nitrobenzene grafted onto Si(001)[41] that useful complementary information can be provided by this method.

The valence electronic structure of the solid bromo- and nitrobenzene multilayers was measured with UPS and explained by comparison to gas phase spectra. The density of states is dominated by the molecular orbitals with only minor modifications from the isolated gas phase state due to molecule−molecule and molecule−adsorbate interaction.

The surface and interface potentials of the formed Si(111)/C_6H_4−X heterostructures were analyzed in terms of the surface band bending (induced by surface states in the forbidden band gap) and surface dipole moment of the adsorbate layer. A lowering of the surface electron affinity was found for the methoxybenzene grafted surface with a surface dipole of −0.33(15) eV which is consistent with the oriented attachment of methoxybenzene. However, the band bending of this surface is still high with about ~0.6 eV. For nitro- and bromobenzene layers, potential steps of +0.36(15) and +0.33(15) eV at the surface were measured, which is consistent with an increase of the electron affinity by the oriented attachment of the molecular dipoles. Also, the interface state-related band bending in silicon was small (~0.1 eV) for the nitro- and bromobenzene grafted surfaces. This indicated that the function of the adsorbed aryl layer is not only electrostatic, increasing the surface electron affinity, but also effects the electronic passivation of the silicon/aryl interface. Nonetheless, a significant amount of interfacial oxides was observed for the silicon surfaces functionalized by aryl groups. Future studies should focus on the optimization of the deposition process in order to reduce the amount of interfacial oxides and the suppression of multilayer formation.

In terms of methodology, the combined application of UPS and XPS to electrochemically modified silicon surfaces allowed for the construction of complete energy band diagrams and the simultaneous analysis of electronic and chemical surface properties. It could be demonstrated that the analysis of the electronic structure of organic adsorbates by UPS is feasible for wet, electrochemically processed systems, and not only for vacuum adsorbed material.

Acknowledgment. We thank M. Gensch and K. Hinrichs from ISAS Berlin for the fruitful discussions and critical reading of the manuscript. R.H. and W.J. acknowledge the support by the German BMBF (Contract No. 05KSARD/0). A.M. and Y.S. thank the Minerva and Krongold foundations for financial support.

References and Notes

(1) Cohen, R.; Ashkenasy, G.; Shanzer, A.; Cahen, D. Grafting Molecular Properties onto Semiconductor Surfaces. In *Semiconductor Electrodes and Photoelectrochemistry*; Bard, A. J., Stratmann, M., Licht, S., Eds.; Wiley: 2002; p 127.

(2) Wolkow, R. A. *Annu. Rev. Phys. Chem.* **1999**, *50*, 413.

(3) Vilan, A.; Shanzer, A.; Cahen, D. *Nature* **2000**, *404*, 166.

(4) Bansal, A.; Li, X.; Lauermann, I.; Lewis, N. S.; Yi, S. I.; Weinberg, W. H. *J. Am. Chem. Soc.* **1996**, *118*, 7225

(5) Linford, M. R.; Chidsey, C. E. D. *J. Am. Chem. Soc.* **1993**, *115*, 12631

(6) Henry de Villeneuve, C.; Pinson, J.; Bernard, M. C.; Allongue, P. *J. Phys. Chem. B* **1997**, *101*, 2415.

(7) Allongue, P.; Henry de Villeneuve, C.; Pinson, J.; Ozanam, F.; Chazalviel, J. N.; Wallart, X. *Electrochim. Acta* **1998**, *43*, 2791.

(8) Hartig, P.; Rappich, J.; Dittrich, T. *Appl. Phys. Lett.* **2002**, *80*, 67.

(9) Hartig, P.; Dittrich, T.; Rappich, J. *J. Electroanal. Chem.* **2002**, *524*−*525*, 120.

(10) Gokhale, S.; Trischberger, P.; Menzel, D.; Widdra, W.; Droge, H.; Steinruck, H.-P.; Birkenheuer, U.; Gutdeutsch, U.; Rosch, N. *J. Chem. Phys.* **1998**, *108*, 5554.

(11) Carbone, M.; Piancastelli, M. N.; Casaletto, M. P.; Zanoni, R.; Comtet, G.; Dujardin, G.; Hellner, L. *Phys. Rev. B* **2000**, *61*, 8531−8536.

(12) Jaegermann, W. The Semiconductor/Electrolyte Interface: A Surface Science Approach; In *Modern Aspects of Electrochemistry*; White, R. E., Conway, B. E., Bockris, J. O. M., Eds.; Plenum Press: New York, 1996; Vol. 30.

(13) Higashi, G. S.; Chabal, Y. J.; Trucks, G. W.; Raghavachari, K. *Appl. Phys. Lett.* **1990**, *56*, 656.

(14) Rappich, J.; Merson, A.; Roodenko, K.; Dittrich, T.; Gensch, M.; Hinrichs, K.; Shapira, Y. *J. Phys. Chem. B* **2006**, *110*, 1332.

(15) Moulder, J. F.; Stickle, W. F.; Sobol, P. E.; Bomben, K. D. *Handbook of X-ray photoelectron scpectroscopy*; Physical Electronics, Inc.: Eden Prairie, MN, 1995.

(16) Distefano, G.; Guerra, M.; Jones, D.; Modelli, A.; Colonna, F. P. *Chem. Phys.* **1980**, *52*, 389.

(17) D'Amours, M.; Belanger, D. *J. Phys. Chem. B* **2003**, *107*, 4811.

(18) Bernard, M.-C.; Chausse, A.; Cabet-Deliry, E.; Chehimi, M. M.; Pinson, J.; Podvorica, F.; Vautrin-Ul, C. *Chem. Mater.* **2003**, *15*, 3450.

(19) Carlson, T. A. *Photoelectron and Auger spectroscopy*; Plenum Press: New York, 1975.

(20) Fujisawa, S.; Ohno, K.; Masuda, S.; Harada, Y. *J. Am. Chem. Soc.* **1986**, *108*, 6505.

(21) Chin, W. S.; Mok, C. Y.; Huang, H. H.; Masuda, S.; Kato, S.; Harada, Y. *J. Electron Spectrosc. Relat. Phenom.* **1992**, *60*, 101.

(22) Yeh, J. J.; Lindau, I. *At. Data Nucl. Data Tables* **1985**, *32*, 1.

(23) Lewerenz, H. J.; Jungblut, H.; Rauscher, S. *Electrochim. Acta* **2000**, *45*, 4615.

(24) Hunger, R.; Mersan, A.; Shapira, Y.; Rappich, J. Unpublished data.

(25) *Practical Surface Analysis by Auger and X-ray Photoelectron Spectroscopy*, 1st ed.; Briggs, D., Seah, M. P., Eds.; Wiley: Chichester, U.K., 1983.

(26) Tanuma, S.; Powell, C. J.; Penn, D. R. *Surf. Interface Anal.* **1993**, *21*, 165.

(27) Seah, M. P.; Gilmore, I. S.; Spencer, S. J. *J. Electron Spectrosc. Relat. Phenom.* **2001**, *120*, 93.

(28) Band, I. M.; Kharitonov, Y. I.; Trzhaskovskaya, M. B. *At. Data Nucl. Data Tables* **1979**, *23*, 443.

(29) Anariba, F.; DuVall, S. H.; McCreery, R. L. *Anal. Chem.* **2003**, *75*, 3837.

(30) Brooksby, P. A.; Downard, A. J. *Langmuir* **2004**, *20*, 5038.
(31) Allongue, P.; Henry de Villeneuve, C.; Cherouvrier, G.; Cortes, R.; Bernard, M.-C. *J. Electroanal. Chem.* **2003**, *550*−*551*, 161.
(32) Brooksby, P. A.; Downard, A. J. *Langmuir* **2005**, *21*, 1672.
(33) Combellas, C.; Kanoufi, F.; Pinson, J.; Podvorica, F. I. *Langmuir* **2005**, *21*, 280.
(34) Pinson, J.; Podvorica, F. *Chem. Soc. Rev.* **2005**, *34*, 429.
(35) Allongue, P.; Delamar, M.; Desbat, B.; Fagebaume, O.; Hitmi, R.; Pinson, J.; Saveant, J.-M. *J. Am. Chem. Soc.* **1997**, *119*, 201.
(36) Sze, S. M. *Physics of Semiconductor Devices*, 2nd ed.; Wiley: New York, 1981.
(37) Himpsel, F. J.; Hollinger, G.; Pollak, R. A. *Phys. Rev. B* **1983**, *28*, 7014.
(38) Flietner, H. *Surf. Sci.* **1988**, *200*, 463.
(39) Lewerenz, H. J.; Aggour, M.; Murrell, C.; Kanis, M.; Jungblut, H.; Jakubowicz, J.; Cox, P. A.; Campbell, S. A.; Hoffmann, P.; Schmeisser, D. *J. Electrochem. Soc.* **2003**, *150*, E185.
(40) Hinrichs, K.; Roseler, A.; Gensch, M.; Korte, E. H. *Thin Solid Films* **2004**, *455*−*456*, 266.
(41) Gensch, M.; Roodenko, K.; Hinrichs, K.; Hunger, R.; Güell, A. G.; Merson, A.; Schade, U.; Shapira, Y.; Dittrich, T.; Rappich, J.; Esser, N. *J. Vac. Sci. Technol., B* **2005**, *23*, 1838.